Stochastic Lorenz dynamics and the mean wind reversals in Rayleigh-Bénard Convection

Yanni L. Bills [1] John S. Wettlaufer [1 2]

[1]Yale University [2]Nordita, Royal Institute of Technology and Stockholm University

Introduction

The Lorenz equations [1] are a severe Galerkin-truncation of the Oberbeck-Boussinesq (OB) equations describing Rayleigh-Bénard convection (RBC). Here, we examine the mathematical connections between the chaotic lobe-switching behavior of the stochastic Lorenz equations and the mean wind reversals in the experiments of Sreenivasan et al. [3]. Long-time numerical simulations, not easily accessible with the OB equations, yield a probability distribution for lobe inter-switch timings that exhibits non-Gaussian, multifractal behavior, whereas in the Gaussian frequency range we mirror the laboratory measurements. The classical Hurst exponent and quadratic variation reveal Brownian second-moment statistics. This demonstrates that the stochastic Lorenz system is a faithful, low-dimensional surrogate for mean-wind reversals in RBC.

Stochastic Model

We force the Lorenz-63 equations [1] with a Gaussian white noise process ξ and amplitude $\hat{\alpha}$ viz.,

$$\frac{dX}{dt} = \sigma(Y - X), \quad \frac{dY}{dt} = X(\rho - Z) - Y, \quad \frac{dZ}{dt} = -\beta Z + XY + \hat{\alpha}\xi(t), \tag{1}$$

where X is the direction and intensity of the convective roll, Y (Z) is the deviation from linearity of the horizontal (vertical) temperature profile, σ is the Prandtl number, ρ is the reduced Rayleigh number, and β is a geometric parameter. The system is ergodic and admits at least one stationary measure [2].

Reversal Tracking

In Sreenivasan et al.'s data, the mean-wind shows chaotic direction reversals [3]. They define T_n as the time between 0 and the n^{th} such reversal, which is shown to be approximately linear in n. Its deviation from linearity (investigated, but not explicitly named, in Ref. [3]) is given by

$$G_n = T_n - (a\,n + b), \tag{2}$$

which is a stochastic process. Analogously we compute G_n by tracking sign-changes of X, which encode convective roll reversals. The power spectral density (PSD) of G_n, both experimentally and numerically, yields a PSD decay scaling of approximately -2.

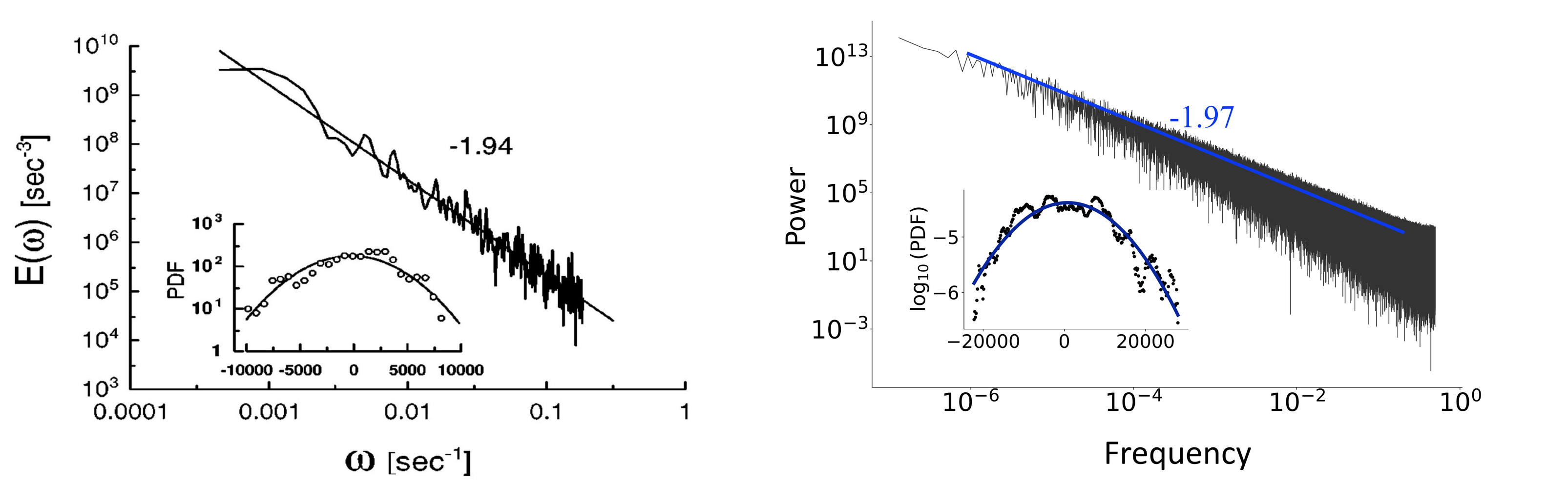

Figure 1. The PSD of G_n from Sreenivasan et al. [3] (left) and our numerical runs (right). The insets show probability distribution functions (PDF) with the expected Gaussian-fit quadratics.

While our PSD has the signature Gaussian scaling, our raw PDF is not Gaussian as in Ref. [3]. However, restricting our G_n to the frequency range $[10^{-4}, 10^{-2}]$ yields a Gaussian PDF.

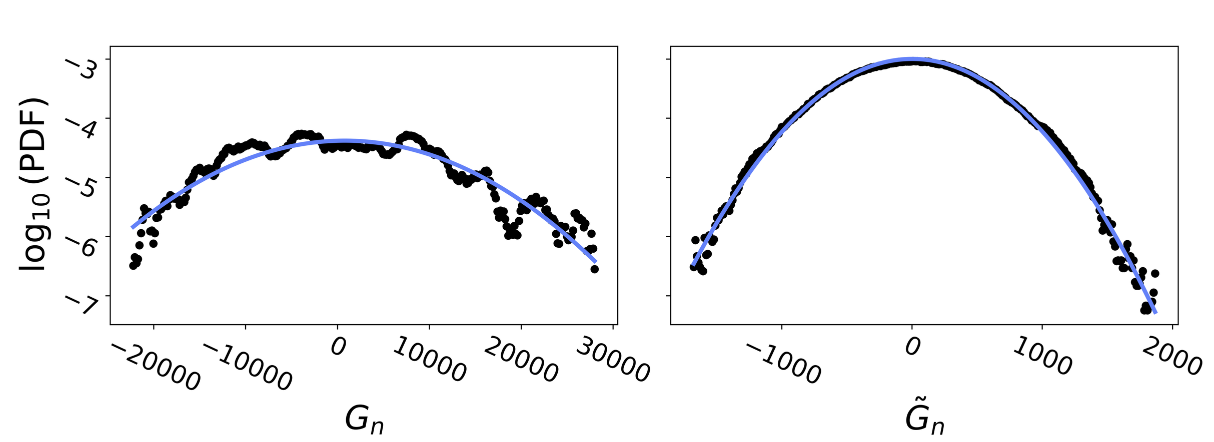

Figure 2. The unfiltered PDF for G_n (left) compared to the filtered $\tilde{G}_n$ PDF (right).

Second Moment Testing

The local Hurst exponent autocovariance function (ACVF) indicates that G_n is a fractional Brownian motion. Its time-averaged mean square displacement (TAMSD) as a function of lag, Δ, is

$$\text{TAMSD}(\Delta) = \frac{1}{N-\Delta}\sum_{n=1}^{N-\Delta}(G_{n+\Delta} - G_n)^2, \tag{3}$$

yielding the classical Hurst exponent, H, through TAMSD(Δ) $\propto \Delta^{2H}$.

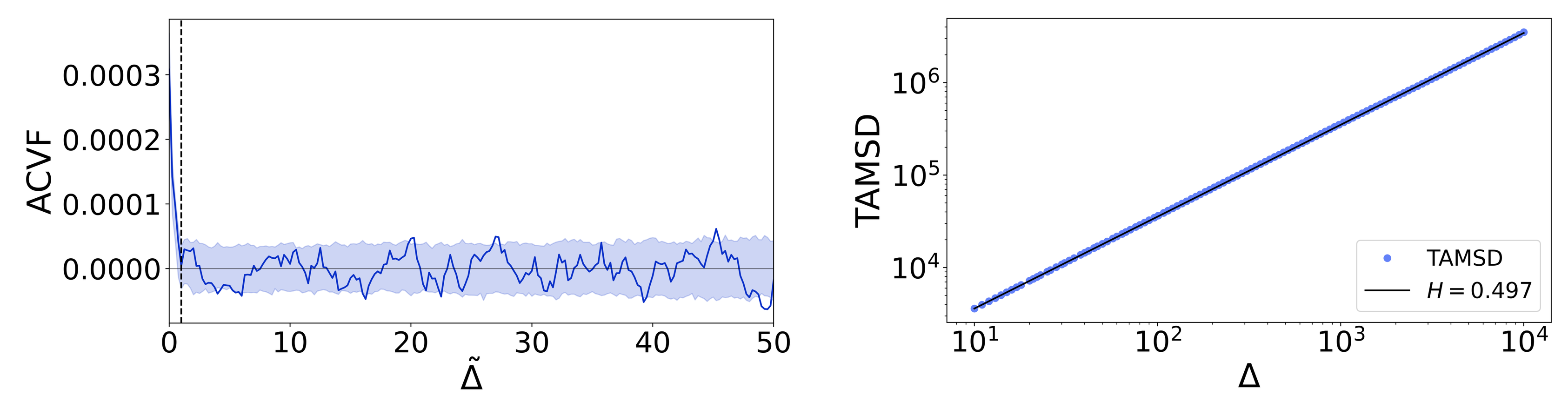

Figure 3. The local H ACVF (left) paired with the TAMSD and its global H estimate.

A Hurst exponent of $H \approx 0.5$ is defined by a Wiener process.

Multifractal Analysis

Key Formulae

We divide the full G_n time series of length N into $\lfloor N/\ell \rfloor$ non-overlapping blocks using scales ℓ. The imposed measure, for some block $B_j(\ell)$, is defined by

$$\mu[B_j(\ell)] = \frac{\sum_{n \in B_j(\ell)} |G_n|}{\sum_{\hat{n}=1}^{N} |G_{\hat{n}}|}, \tag{4}$$

from which the q-moment partition function is defined by

$$\chi(q,\ell) = \sum_j \left(\mu[B_j(\ell)]\right)^q \overset{\ell \to 0}{\sim} \ell^{\tau(q)}. \tag{5}$$

The mass-scaling exponent, $\tau(q)$, is equivalent to $(q-1)D_q$, where D_q are the Rényi dimensions. A Legendre transform connects $\tau(q)$ to the Hölder exponent, $\alpha(q)$, and the multifractal spectrum, $f(\alpha) := q\alpha(q) - \tau(q)$ [4].

Numerical Estimates

It is found that $\tau(q)$ admits a spectrum that is non-linear in q, which exhibits multifractality in G_n. The Rényi dimensions and multifractal spectrum follow suit.

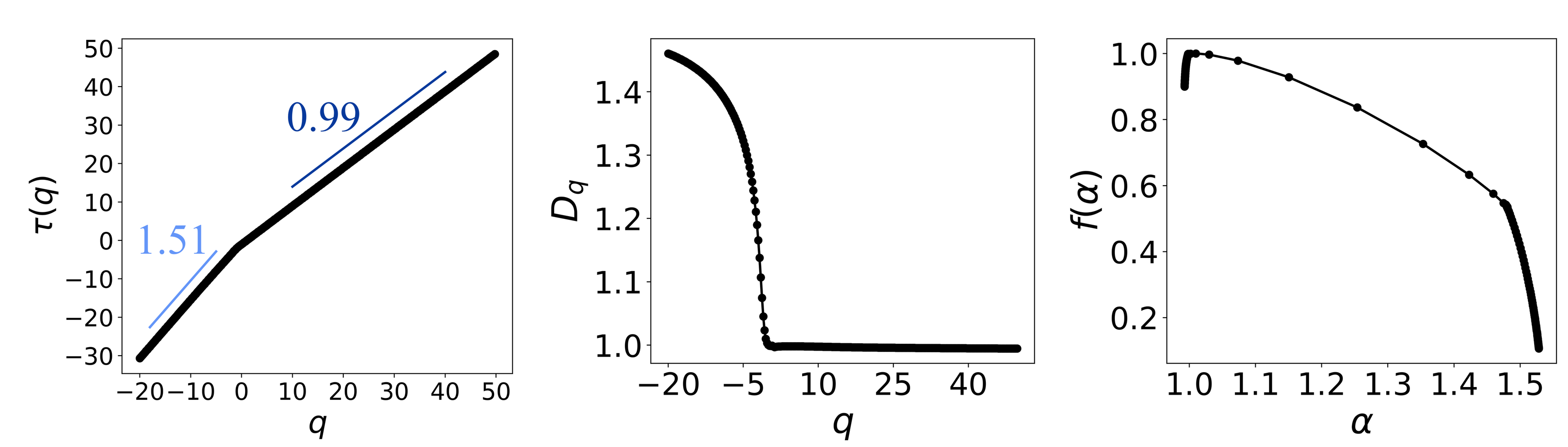

Figure 4. The mass-scaling exponent, $\tau(q)$, plotted against each realized moment with the differing slopes fitted with blue lines (left). The Rényi dimensions are plotted against each moment q (center) and the multifractal spectrum is shown for the full range of realized Hölder exponents (right).

Cantor Cascade

The chosen measure, μ, assigns large density to large magnitude inter-switch timing deviations and small density to the high-frequency oscillation about the linear trend. To replicate the multifractal behavior of G_n with an analytic formulation, we enact a Cantor set cascade that begins from a unit-length support.

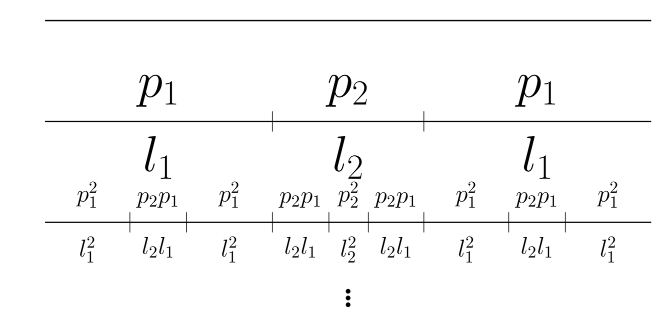

Figure 5. The three-pronged Cantor set cascade showing the pattern of fractal iteration.

We define two equivalent branches of larger mass that correspond to large bursts in G_n, while a central, smaller mass branch corresponds to high-frequency scatter about the mean. Accordingly, $2p_1 + p_2 = 1$ ($2l_1 + l_2 = 1$), such that $p_1 > p_2$ ($l_1 > l_2$). It follows that the covering count, $N(l_n)$, gives values for both α and $f(\alpha)$ for a cascade of $n = n_1 + n_2$ steps with n_1 type p_1 steps and n_2 type p_2 steps via

$$N(l_n) = 2^{n_1}\binom{n}{n_1} \sim l_n^{-f(\alpha)}, \quad \text{and} \quad \alpha = \lim_{n\to\infty}\frac{\log p_n}{\log l_n}. \tag{6}$$

Here, $p_n = p_1^{n_1}p_2^{n_2}$ and $l_n = l_1^{n_1}l_2^{n_2}$.

The mass-scaling spectrum, Rényi dimensions, and multifractal spectrum are recreated; they exhibit good agreement with the numerically estimated versions.

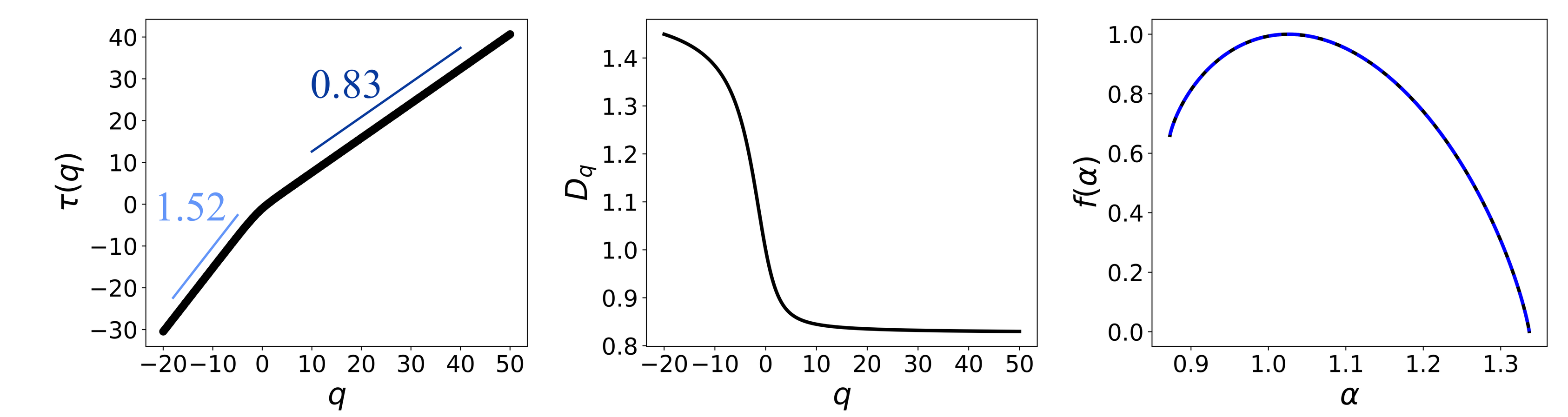

Figure 6. Analytic $\tau(q)$ (left), D_q (center), and $f(\alpha)$ (right) with $l_1 = 0.35$, $p_1 = 0.4$.

Summary

- Sampling the numerical frequencies within a particular range acts to "Gaussianize" data by foregoing high-frequency jitter and low-frequency undulation showing how central limit theorem effects dominate.
- The inter-switch timing process, G_n, is a Wiener process at second moment.
- The inter-switch process is a multifractal and has temporally non-uniform singularity scaling that can be replicated by an analytic Cantor cascade formalism.
- The results provide a simple quantitative framework for experiments of Sreenivsan et al. [3].

References

[1] E.N. Lorenz, "Deterministic nonperiodic flow", *J. Atmos. Sci.* **20** (1963) 130–141.

[2] M. Coti Zelati, M. Hairer, "A Noise-Induced Transition in the Lorenz System", *Commun. Math. Phys.* **383** (2021) 2243–2274.

[3] K. R. Sreenivsan, A. Bershadskii, J. J. Niemela, "Mean wind and its reversal in thermal convection", *Phys. Rev. E* **65** (2002) 056306.

[4] B. Mandelbrot, "An Introduction to Multifractal Distribution Functions", in H. Stanley and N. Ostrowsky (Eds.), *Fluctuations and Pattern Formation:* Kluwer Academic, Dordrecht, 1988, pg. 279–291